The graph-theoretic minimum energy path problem for ionic conduction

The graph-theoretic minimum energy path problem for ionic conduction

Ippei Kishida

The graph-theoretic minimum energy path problem for ionic conduction

Cite as: AIP Advances **5**, 107107 (2015); https://doi.org/10.1063/1.4933052
Submitted: 25 August 2015 . Accepted: 28 September 2015 . Published Online: 07 October 2015

Ippei Kishida

AIP ADVANCES **5**, 107107 (2015)

The graph-theoretic minimum energy path problem for ionic conduction

Ippei Kishida[a]
Department of Mechanical Engineering, Osaka City University, Sumiyoshi, Osaka 558–8585, Japan

(Received 25 August 2015; accepted 28 September 2015; published online 7 October 2015)

A new computational method was developed to analyze the ionic conduction mechanism in crystals through graph theory. The graph was organized into nodes, which represent the crystal structures modeled by ionic site occupation, and edges, which represent structure transitions via ionic jumps. We proposed a minimum energy path problem, which is similar to the shortest path problem. An effective algorithm to solve the problem was established. Since our method does not use randomized algorithm and time parameters, the computational cost to analyze conduction paths and a migration energy is very low. The power of the method was verified by applying it to α-AgI and the ionic conduction mechanism in α-AgI was revealed. The analysis using single point calculations found the minimum energy path for long-distance ionic conduction, which consists of 12 steps of ionic jumps in a unit cell. From the results, the detailed theoretical migration energy was calculated as 0.11 eV by geometry optimization and nudged elastic band method. Our method can refine candidates for possible jumps in crystals and it can be adapted to other computational methods, such as the nudged elastic band method. We expect that our method will be a powerful tool for analyzing ionic conduction mechanisms, even for large complex crystals. [http://dx.doi.org/10.1063/1.4933052]

INTRODUCTION

Various theoretical and computational approaches have contributed to the development of new superionic conductors, which are a key issue for devices such as fuel cells, batteries, and sensors. First-principles calculation is a powerful tool for analyzing defect formation and conduction mechanisms.[1–11] Although first-principles calculations with the nudged elastic band method (NEBM) can reveal a trajectory and an activation energy between two particular states,[12–15] the whole conduction path must be assumed before the calculations. First-principles molecular dynamics (FPMD) simulates atomic behaviors in complex crystals at finite temperatures.[16–22] However, the method requires a large amount of computational resources, complicated analysis, and sensible parameters for time steps and measurement times. Kinetic Monte Carlo method[23,24] is an effective approach to find candidates of the saddle points of ionic conduction. But the method also needs sensible parameters for time step and atomic displacement. In addition, it does not guarantee reaching the true saddle point because the method uses randomized algorithm. A new approach is required to model crystal state transitions easily and effectively.

Ionic conduction mechanism

Ionic conduction in crystals typically arises via lattice defects, that is, vacancies and interstitials. In any case, movement of ions between sites plays an important role. Macroscopic diffusion constant at a given temperature T, $D(T)$, can be estimated according to

[a]kishida@imat.eng.osaka-cu.ac.jp

$$D(T) = a^2 \nu \exp(-E_m/k_B T) \quad (1)$$

where a is the hopping distance, ν is the hopping frequency, E_m is the migration energy, and k_B is Boltzmann's constant.[15,25] Because the equation is an exponential function of E_m with $a^2\nu$ as a pre-exponential factor, E_m is generally more important than a and ν.

Minimum energy path problem

The migration energy, E_m, is decided by the energy at the saddle point of conduction. Strict systematization of ionic occupation and transition via graph theory can aid the finding the saddle point of ionic conduction in various crystals. This method is widely used to distinguish crystal structures by differences in occupied sites and to elucidate conduction mechanisms. However, the full potential of this technique is not widely appreciated. Most ionic crystals have frame structures of counterions with larger ionic radii and interstitial ions with smaller ionic radii. Assuming the frame structure is homogeneous, the whole crystal structure can be expressed by using a combination of occupied sites. The combination can be treated as a node in graph theory (Fig. 1). An ion in the crystal may jump to neighboring interstitial sites. These jumps correspond to a transition of the combination, and this is modeled as edges in the graph (Fig. 1(b)). Although the word 'path' usually refers to an ion trajectory, it is redefined in the present study as the transition of a whole crystal state, the ions of which travel long distances. Although the actual conduction path is composed of these transitions, the number of possible paths can easily produce a combinatorial explosion. Ionic conductivity dominantly depends on the minimum energy path (MEP), which is the path with the lowest migration energy among possible paths. We propose the minimum energy

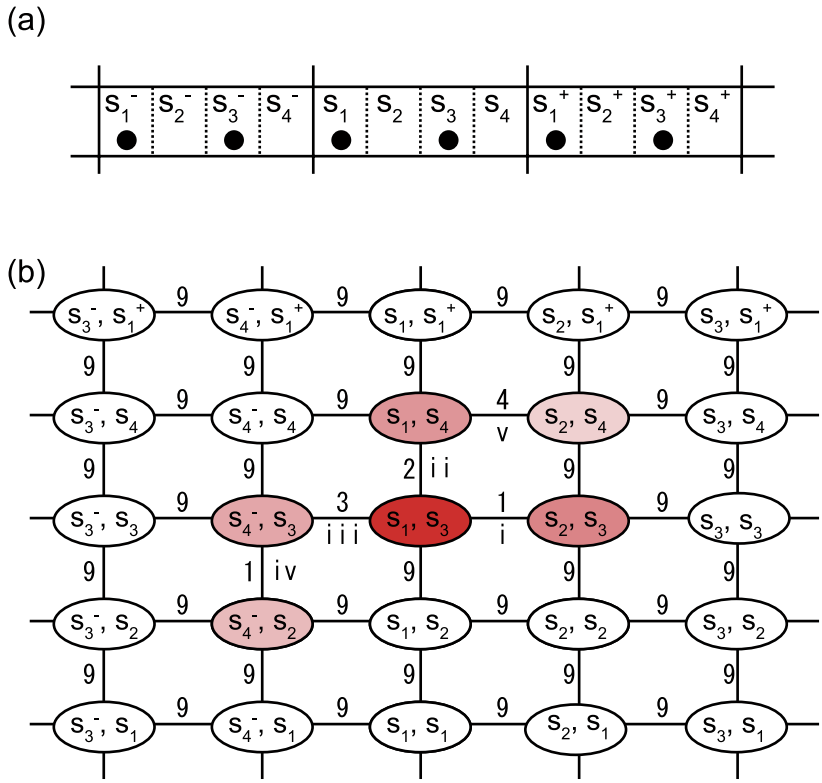

FIG. 1. Schematic image of the MEPP. (a) One-dimensional crystal with four sites in a unit cell. s_i indicates site names. Two closed circles in each cell indicate the ion occupation in the initial state. Superscript + and − of s_i indicate that the sites exist in a cell other than the initial cell. (b) Graph surrounding the (s_1, s_3) node (red online). Circles indicate the occupied site set(OSS). Lines indicate transition of the OSS. Arabic numbers along the edges indicate the weights as the migration energy of the transition. Lower case Roman numerals indicate the order of expansion of the nodes reached (red online, darker shading indicates earlier expansion).

path problem (MEPP), which consists of identifying the MEP in a weighted graph. The MEPP is similar to the shortest path problem (SPP), which is a basic problem in graph theory,[26] but there are some differences. The purpose of the SPP is to find the path that minimizes the sum of the edge weights, whereas that of MEPP is to find the path that minimizes the maximum of the edge weights. In addition, although simple SPP can assume only one destination, MEPP has multiple destinations in all directions in a crystal. Therefore, Dijkstra's algorithm, which is often used for SPP, cannot be applied to MEPP.

METHODOLOGY

In this paper, we present a method based on graph theory to find an MEP in a crystal. We assume that there are m sites for interstitials, $s_i (1 \leq i \leq m)$, in a unit cell. The combination of occupied sites of n ions in the cell is called the occupied site set (OSS). Each OSS, expressed by v_j as a node, has occupied sites $(s_{j1}, s_{j2}, \ldots, s_{jn})$ and its own energy $E(v_j)$. Because the order of occupied sites is unimportant, for arbitrary j, k, l,

$$v_j = (\cdots, s_{jk}, \cdots, s_{jl}, \cdots) = (\cdots, s_{jl}, \cdots, s_{jk}, \cdots).$$

Fig. 1 shows schematic images of a one-dimensional crystal with $m = 4$ and $n = 2$.

Algorithm

We assume that the starting OSS v_{start} is (s_1, s_3), an ion can jump to neighboring sites, and that the weights of all edges are already known. Long distance conduction occurs when the path connects one OSS to another crystallographically equivalent OSS that includes an ion outside the initial cell. OSSs with this relationship are called quasi-equivalent OSSs (qe-OSSs). An algorithm to solve the MEPP is as follows.

(I) Add arrival attribute to v_{start}.
(II) List all edges that connect two nodes with and without arrival attribute (hereafter called hetero-arrival edges).
(III) Choose the hetero-arrival edge with the lowest weight as the next passing edge.
(IV) Add arrival attribute to the node behind the next passing edge (hereafter called the next node).
(V) Make the next node store the previous node behind the next passing edge.
(VI) If the next node is the qe-OSS of any node with the arrival attribute, break the exploration loop.
(VII) Repeat from (II) to (VI).

After the loop is broken, a pair of nodes, comprising an OSS and its qe-OSS, is obtained; OSS (s_4^-, s_2) and (s_2, s_4) in Fig. 1. Each of the OSSs can be elevated to v_{start} by using its stored data. An MEP that connects v_{start} and qe-OSS of v_{start} can be composed of two paths: v_{start} to one node of the obtained pair and the inverse transition of the path from v_{start} to the other node.

α-AgI

We apply this method to α-AgI, which is one of the earliest superionic conductors.[27–30] Previous studies showed that its superionicity results from the existence of many vacant interstitial sites in its body-centered cubic (bcc) structure.[31,32] However, there are few studies that explain the superionic conduction mechanism quantitatively. Although the high symmetry of α-AgI is an advantage for obtaining precise information via first-principles calculations, it is also a disadvantage for detailed identification of the crystal structure. The presented method is suitable for complex crystals because it is highly systematized through strict definitions and can be programmed in computers. Some supplemental assumptions are made to solve MEPP in α-AgI. We assume that at most one Ag ion can jump to neighboring sites at each step. The higher energy of both terminal OSSs of an edge is used as a weight (the migration energy) of the edge in the MEPP analysis because structures with higher energies tend to have a higher migration energy.

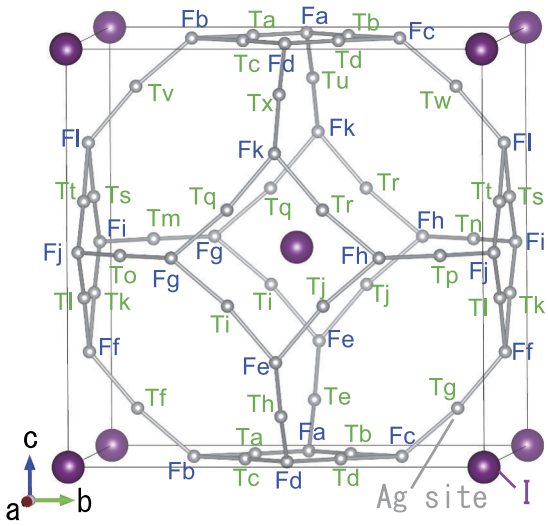

FIG. 2. Unit cell of α-AgI. Small (gray online) and large (purple online) spheres indicate Ag and I ion sites, respectively. Bonds between Ag ions indicate the first-nearest neighbor relationship. Fa, ⋯, Fx (green online), Ta, ⋯, Tl (blue online), are labels for each Ag site.

Fig. 2 shows a prototype of the crystal structure of α-AgI with all Ag sites. We use the following crystallographic data for α-AgI, as reported by Cooper:[33] space group $Im\bar{3}m$ with lattice constants $a = b = c = 5.062$ [Å] and $\alpha = \beta = \gamma = 90$[°]. A unit cell of α-AgI has two Ag ions in the I sublattice with a bcc structure. There are F and T Ag sites in α-AgI. The F sites are close to four T sites and the T sites are close to two F sites. A unit cell contains 12 F sites and 24 T sites, and these sites are labeled in Fig. 2. We assume that Ag ions occupy these 36 sites exclusively. Although there are ${}_{36}C_2 = 630$ variations of OSSs with simple combinations, there are 19 crystallographically distinct OSSs with 96 symmetry operations of $Im\bar{3}m$. (Table I).

First-principles calculations

The calculations are performed by using density functional theory[34,35] with the plane-wave projector augmented-wave method[36] as implemented in the VASP code.[37–39] The exchange-correlation term is treated with the Perdew-Burke-Ernzerhof functional[40] based on the generalized gradient approximation. The plane-wave cutoff energy is 500 eV, and k-point sampling is conducted at $8 \times 8 \times 8$ points from the preliminary calculations to evaluate the precision of the total energy. Single-point calculations (SPCs) and geometry optimizations (GOs) are performed. In the GOs, the ionic positions are relaxed until the residual forces are less than 0.02 eV/Å, with the lattice constants fixed at the values obtained from preliminary calculations, $a = 5.117$ Å, which overestimates the experimentally obtained value of $a = 5.062$ Å[33] by 1.0 %. Occupied sites after GO are distinguished as the nearest site in a periodic cell among the 36 sites. Energy profiles between two stable structures are performed by using NEBM with repeated bisection into eight segments.[11]

RESULTS AND DISCUSSIONS

Single point calculations and geometry optimizations

Table I shows the total energies of SPCs and GOs for 19 unique initial structures. Because GO altered the OSSs of 11 initial structures, the energies of these structures were not those of the initial OSSs and could not be used for conduction path analysis. The eight other OSSs consisted of F-F or T-T combinations, not F-T combinations. Because F and T sites neighbor only T and F sites, respectively, F-F and T-T combinations must transit via F-T combination in a conduction path.

TABLE I. Energies of unit cell of α-AgI relative to the lowest value, E_{geom}(Fa, Fj). E_{SPC} and E_{GO} are energies obtained from SPCs and GOs, respectively. Symbol '–' in E_{geom} indicates that the energy cannot be obtained because the OSS was changed during GO. $\mathrm{OSS_{init}}$ and $\mathrm{OSS_{GO}}$ indicate the OSSs of the initial state of calculation and that of final state after GO, respectively. Symbol '–' in $\mathrm{OSS_{GO}}$ indicates that the OSS after GO is the same as the initial state, $\mathrm{OSS_{init}}$. d indicates distance between Ag ions in the periodic cell in the initial state.

label	$\mathrm{OSS_{init}}$	E_{SPC}[eV]	E_{GO}[eV]	$\mathrm{OSS_{GO}}$	d [Å]
v_{19}	(Fa, Ta)	124.28	–	(Fa, Tf)	0.90
v_{18}	(Ta, Tb)	43.03	–	(Fa, Fd)	1.16
v_{17}	(Ta, Te)	15.37	–	(Fa, Ff)	1.60
v_{16}	(Ta, Td)	13.28	1.82	–	1.65
v_{15}	(Fa, Fb)	7.81	0.73	–	1.79
v_{14}	(Fa, Tc)	4.73	–	(Fa, Tf)	1.79
v_{13}	(Fa, Fd)	0.79	0.79	–	2.53
v_{12}	(Fa, Tf)	0.78	–	(Fa, Ff)	2.40
v_{11}	(Ta, Tg)	0.66	–	(Fa, Ff)	2.66
v_{10}	(Ta, Ti)	0.60	–	(Fa, Fi)	2.76
v_9	(Ta, Tm)	0.53	0.16	–	3.18
v_8	(Ta, Tj)	0.48	–	(Fa, Fj)	2.99
v_7	(Ta, Tn)	0.37	–	(Fa, Fj)	3.83
v_6	(Fa, Tk)	0.34	–	(Fa, Ff)	3.27
v_5	(Ta, Tp)	0.31	0.31	–	4.38
v_4	(Fa, Tl)	0.21	–	(Fa, Fj)	3.69
v_3	(Fa, Fi)	0.20	0.12	–	3.58
v_2	(Fa, Ff)	0.11	0.04	–	3.10
v_1	(Fa, Fj)	0.00	0	–	4.38

However, there were no stable F-T combination for GO. Therefore, a conduction path could not be created from the GO results. However, SPCs can obtain the OSS energies even when the ions are not surrounded by a potential barrier. Among the eight OSSs, the energies obtained from the SPCs, E_{SPC}, showed qualitatively good agreement with those from GOs, E_{GO}. SPC was more suitable than GO for simple analysis of conduction paths in the present study.

OSS v_1 (Fa, Fj) was the most stable in both calculations; therefore, it was expected to be the base state of conduction. F sites tend to have lower energies than T sites. Structures with longer distances between Ag ions, d in Table I, tend to have lower energy because of the electrostatic interactions. There results agree well with previous reports.[32]

Solving minimum energy path problem

All the conditions and data to apply our method were obtained, and we calculated an MEP. Fig. 3 shows a limited number of nodes neighboring the MEP for clarity because more than 200 nodes appeared before the MEP was found. The exact ionic sites in the surrounding cells were described in the style of a crystallographic information file (CIF);[41] three digits with a value out of 5 indicated the cell allocation. For example, '564' indicates an atom located in a cell of [0, +1, −1] with internal coordinates from a center cell. Starting from v_{1a}, the OSS transition followed $v_{1a} \rightarrow v_{4a} \rightarrow \cdots \rightarrow v_{2c}$ and $v_{1a} \rightarrow v_{4h} \rightarrow \cdots \rightarrow v_{2d}$ along the thick lines on the left- and right-hand sides of Fig. 3, respectively. Because v_{2d} (Fl564, Fg655) was a qe-OSS of v_{2c} (Fg555, Fl555), the conduction path formed an imaginary helix, shown as a circuit owing to the projection in Fig. 3. v_{2d} was adjusted to v_{2c} by exchanging the first and second Ag sites, and shifting the cell allocation by [−1, 0, 0] for an Fg site and by [0, −1, +1] for an Fl site. Applying this procedure to all nodes in the right half of Fig. 3, v_{1a} (Fa555, Fj555) reached (Fj455, Fa546), which is a qe-OSS of v_{1a}, by the counterclockwise route in Fig. 3. An animation of this conduction process is provided as Fig. S1 in supplemental material.[42] The highest energy of the OSSs along the MEP was +0.21 eV. This energy corresponded roughly to the migration energy.

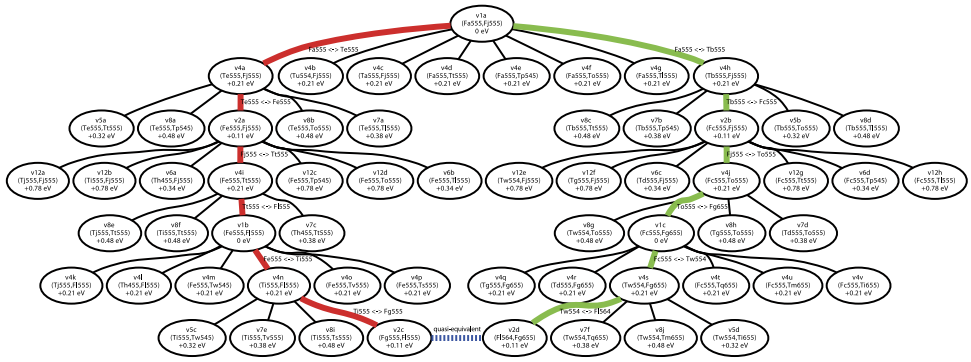

FIG. 3. MEP and neighboring OSSs of α-AgI. Circles indicate nodes, which include an identical label, the site occupation of two Ag ions, and energy. The integer following v in the label corresponds to a class of symmetrically equivalent OSSs in Table I. The site occupation with three digits is in the same format as a crystallographic information file (CIF).[41] Site changes of transitions on an MEP are shown to the right of edges on the path. Two thick lines (red and green online) indicate the two parts of the MEP. The broken thick line (blue online) indicates the qe-OSS relationship of the nodes.

True saddle point using NEB method

To obtain the true migration energy, accurate transition energies are required. Because the MEP consisted of a sequence of symmetrically equivalent OSSs, that is, $v_1 \rightarrow v_4 \rightarrow v_2$, and its inversion, this process determined the migration energy of α-AgI. It was difficult to use NEBM for the $v_1 \rightarrow v_4$ and $v_4 \rightarrow v_2$ transition owing to the instability of v_4 for GO. However, NEBM could be applied to the $v_1 \rightarrow v_2$ transition, because the location of the Fa, Te, and Fe sites was almost linear. Fig. 4 shows the energy profile between v_{1a} and v_{2a}. Because the energy profile had a single peak, there was no stable site between Fj and Fi. This is consistent with the results in Table I, namely v_4 (Fa, Tl) converged to v_1 (Fa, Fj) by GO. The migration energy was obtained as 0.11 eV. Here, the possibility of a different MEP that excludes the nodes v_1, v_2, and v_4 is discussed. Focusing on stable structures for GO in Table I, all OSSs except for v_1, v_2 have $E_{\mathrm{GO}} > 0.11$ eV. Because the migration energy is higher than energies of the stable structures, the migration energy of the paths that contains these OSSs is not less than 0.11 eV. Among the F-T OSSs, v_6 has the second lowest E_{SPC}. Because this is higher than that of v_4, by 0.13 eV, it is unlikely that the migration energy via v_6 was lower than 0.11 eV even with structure relaxation considered. Therefore, it is unlikely that MEPs other than the path shown in Fig. 3 existed. Consequently, Ag ionic conduction in α-AgI results from the mechanism using the MEP with the migration energy of 0.11 eV. Since this calculated E_{m} is sufficiently low for ionic conduction, this value agrees well with the previous calculation[32] and experimental value.[29] The difference of 0.06 eV between this theoretical value and the experimental value may be caused by a entropy effect, which is not taken into account in the present study. These results also agree well with previous studies on bottle neck of ionic conduction. In addition, the present study reveals a detailed conduction mechanism which consist of precise structure transitions via ionic jumps in a cell.

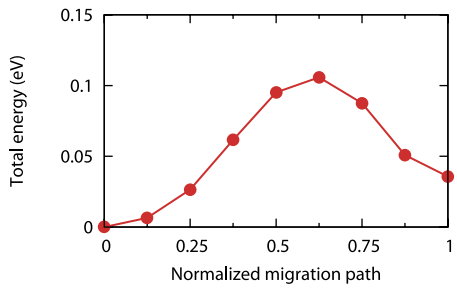

FIG. 4. Energy profile for migration path between v_{1a} ($x = 0$) and v_{2a} ($x = 1$).

Advantage of the method

We discuss the feature and extendibility of our method compared to other methods such as FPMD and KMC. Our method can guarantee reaching the true saddle point within finite amount of calculation if the conduction path exist, that is, the conduction was not isolated by subgraphs. The method has an additive advantage of eliminating the need for difficult adjustment of time step, measurement time, and displacement, which are not essential in physics. As shown in Eq. (1), time factor is included in ν and not included in E_{m}. Although FPMD and KMC use time evolution to obtain the saddle point and E_{m}, our method enables to analyze without using the time factor. Therefore, our method consumes much lower computational costs than FPMD or KMC. The pathway identified from the present algorithm could be used for other computational methods; for example, divided components of the migration path for NEBM demonstrated in the present study and input to FPMD enhanced sampling along collective variable defined by pathway.[43]

Our method is adaptable to various conduction mechanisms in crystals. In the present study, the ionic conduction in α-AgI was derived from the idea based on the interstitial mechanism. Since a unit cell with two interstitials in 36 sites is equal to a unit cell with 34 vacancies, the method obviously has availability to vacancy mechanism for conduction. The assumptions used for α-AgI in the present study can be extended easily. For example, allowing multiple occupation of ions in a site results in additional nodes. Allowing multiple ion jumps at the same time results in additional edges. This modification enables analysis to include interstitialcy mechanism.

Although the present study found only one conduction path in α-AgI, multiple conduction paths can be found by little modification of the algorithm. For example, the finding loop is broken when the energy of the next passing edge becomes higher than setting value at (VI) in the algorithm. Note that these extensions were not adopted and we used the simplest model, since the aim of this study is the verification of the method.

Although it is theoretically desirable that all migration energies between OSSs are obtained before solving the MEPP, it requires a lot of computational resources, and it is effective in practice to use energies obtained from SPCs as preliminary migration energies, as demonstrated in this study.

CONCLUSIONS

We proposed a MEPP based on graph theory and provided an algorithm to solve the problem. By using this method, the ionic conduction mechanism in α-AgI crystal was determined quantitatively. The migration energy along a MEP in α-AgI was found to be 0.11 eV. Because this method can refine candidate jumps in crystals and is well suited to NEBM, we expect our method will be a powerful tool for analyzing ionic conduction mechanisms, even for large and complex crystals.

This work was supported by JSPS KAKENHI Grant Number 26820319.

[1] P. Blaha, K. Schwarz, and P. Herzig, Physical Review Letters **54**, 1192 (1985).
[2] R. Fracchia, G. Barrera, and N. Allan, Journal of Physics and Solids **59**, 435 (1998).
[3] W. Frank, U. Breier, C. Elsässer, and M. Fähnle, Physical review letters **77**, 518 (1996).
[4] M. Catti, Physical Review B **61**, 1795 (2000).
[5] A. Van der Ven, G. Ceder, M. Asta, and P. Tepesch, First-principles theory of ionic diffusion with nondilute carriers, (2001).
[6] Y. Koyama, Y. Yamada, I. Tanaka, S. R. Nishitani, H. Adachi, M. Murayama, and R. Kanno, Mater. Trans. **43**, 1460 (2002).
[7] V. Meunier, J. Kephart, C. Roland, and J. Bernholc, Physical review letters **88**, 075506 (2002).
[8] M. V. Koudriachova, N. M. Harrison, and S. W. de Leeuw, Physical Review B **65**, 235423 (2002).
[9] M. V. Koudriachova, N. M. Harrison, and S. W. D. Leeuw, Solid State Ionics **157**, 35 (2003).
[10] I. Kishida, Y. Koyama, A. Kuwabara, T. Yamamoto, F. Oba, and I. Tanaka, The Journal of Physical Chemistry B **110**, 8258 (2006).
[11] I. Kishida, F. Oba, Y. Koyama, A. Kuwabara, and I. Tanaka, Physical Review B - Condensed Matter and Materials Physics **80**, 24116 (2009).
[12] G. Mills, H. Jónsson, and G. K. Schenter, Surface Science **324**, 305 (1995).
[13] G. Henkelman, H. Jo, and I. Introduction, The Journal of Chemical Physics **113**, 9978 (2000).
[14] X. Ke and I. Tanaka, Physical Review B **69**, 165114 (2004).
[15] H. Moriwake, A. Kuwabara, C. A. J. Fisher, R. Huang, T. Hitosugi, Y. H. Ikuhara, H. Oki, and Y. Ikuhara, Advanced materials (Deerfield Beach, Fla.) **25**, 618 (2013).
[16] G. Kresse and J. Hafner, Physical Review B **47**, 558 (1993).

[17] J. Sarnthein, K. Schwarz, and P. Blöchl, Physical review. B, Condensed matter **53**, 9084 (1996).
[18] C. Ouyang, S. Shi, Z. Wang, X. Huang, and L. Chen, "First-principles study of Li ion diffusion in LiFePO4" (2004).
[19] C. Moysés Araújo, A. Blomqvist, R. Scheicher, P. Chen, and R. Ahuja, "Superionicity in the hydrogen storage material Li2NH: Molecular dynamics simulations" (2009).
[20] Y. Mo and S. P. Ong, Chemistry Of Materials **24**, 15 (2012).
[21] K. Fujimura, A. Seko, Y. Koyama, A. Kuwabara, I. Kishida, K. Shitara, C. A. J. Fisher, H. Moriwake, and I. Tanaka, Advanced Energy Materials **3**, 980 (2013).
[22] R. Jalem, Y. Yamamoto, H. Shiiba, M. Nakayama, H. Munakata, T. Kasuga, and K. Kanamura, Chemistry of Materials **25**, 425 (2013).
[23] A. Bortz, M. Kalos, and J. Lebowitz, Journal of Computational Physics **17**, 10 (1975).
[24] L. Xu and G. Henkelman, The Journal of Chemical Physics **129**, 114104 (2008).
[25] M. W. Barsoum, *Fundamentals of Ceramics (Series in Material Science and Engineering)* (CRC Press, 2002).
[26] R. Gritzmann, Peter, and Brandenberg, *Das Geheimnis des kürzesten Weges* (Springer Boston, 2005).
[27] P. Vashishta and A. Rahman, Physical Review Letters **40**, 1337 (1978).
[28] I. Abrahams, P. G. Bruce, A. R. West, and W. I. F. David, Journal of Solid State Chemistry **75**, 390 (1988).
[29] R. Agrawal, K. Kathal, and R. Gupta, Solid State Ionics **74**, 137 (1994).
[30] S. Hull, Reports on Progress in Physics **67**, 1233 (2004).
[31] R. Cava, F. Reidinger, and B. Wuensch, Solid State Communications **24**, 411 (1977).
[32] S.-r. Sun and D.-g. Xia, Solid State Ionics **179**, 2330 (2008).
[33] M. J. Cooper and M. Sakata, "The interpretation of neutron powder diffraction measurements on α-AgI" (1979).
[34] P. Hohenberg and W. Kohn, Physical Review **136**, B864 (1964).
[35] W. Kohn and L. J. Sham, Physical Review **140**, A1133 (1965).
[36] P. E. Blöchl, Physical Review B **50**, 17953 (1994).
[37] G. Kresse and J. Hafner, Physical Review B **48**, 13115 (1993).
[38] G. Kresse and J. Furthmüller, Physical review B **54**, 11169 (1996).
[39] G. Kresse and D. Joubert, Physical Review B **59**, 1758 (1999).
[40] J. P. Perdew, K. Burke, and M. Ernzerhof, Physical Review Letters **77**, 3865 (1996).
[41] S. R. Hall, F. H. Allen, and I. D. Brown, "The crystallographic information file (CIF): a new standard archive file for crystallography" (1991).
[42] See supplementary material at http://dx.doi.org/10.1063/1.4933052 for animation of conduction process along minimum energy path.
[43] D. Bucher, L. C. T. Pierce, J. A. McCammon, and P. R. L. Markwick, Journal of Chemical Theory and Computation **7**, 890 (2011).